Biomarkers of Migraine and Cluster Headache: Differences and Similarities

Roberta Messina [1,2,3] Carole H. Sudre,[4] Diana Y. Wei,[3] Massimo Filippi [1,2,5]
Sebastien Ourselin,[4] and Peter J. Goadsby[3]

Objective: This study was undertaken to identify magnetic resonance imaging (MRI) biomarkers that differentiate migraine from cluster headache patients and imaging features that are shared.

Methods: Clinical, functional, and structural MRI data were obtained from 20 migraineurs, 20 cluster headache patients, and 15 healthy controls. Support vector machine algorithms and a stepwise removal process were used to discriminate headache patients from controls, and subgroups of patients. Regional between-group differences and association between imaging features and patients' clinical characteristics were also investigated.

Results: The accuracy for classifying headache patients from controls was 80%. The classification accuracy for discrimination between migraine and controls was 89%, and for cluster headache and controls it was 98%. For distinguishing cluster headache from migraine patients, the MRI classifier yielded an accuracy of 78%, whereas MRI–clinical combined classification model achieved an accuracy of 99%. Bilateral hypothalamic and periaqueductal gray (PAG) functional networks were the most important MRI features in classifying migraine and cluster headache patients from controls. The left thalamic network was the most discriminative MRI feature in classifying migraine from cluster headache patients. Compared to migraine, cluster headache patients showed decreased functional interaction between the left thalamus and cortical areas mediating interoception and sensory integration. The presence of restlessness was the most important clinical feature in discriminating the two groups of patients.

Interpretation: Functional biomarkers, including the hypothalamic and PAG networks, are shared by migraine and cluster headache patients. The thalamocortical pathway may be the neural substrate that differentiates migraine from cluster headache attacks with their distinct clinical features.

ANN NEUROL 2023;93:729–742

Primary headaches, like migraine and cluster headache, are among the most common and disabling neurological diseases worldwide.[1] Diagnosis of migraine and cluster headache is mainly based on taking a careful clinical history. Migraine patients usually experience a unilateral or bilateral throbbing pain that might last from 4 to 72 hours, and might be associated with nausea, vomiting, and increased sensitivity to light, sound, and head movement.[2] Core features of cluster headache attacks are the excruciating unilateral pain, lasting from 15 to 180 minutes, cranial autonomic symptoms (CAS), and a sense of

restlessness and agitation. Typically, there are periods when cluster headache patients experience a series of daily headache attacks, known as the "in bout" phase, that may last from 7 days to 1 year. Between one bout and another, patients are completely free from their headache attacks; this period is called the "out of bout" phase.[3]

Although the clinical phenotype of these two primary headaches can be different, they share some pathophysiological mechanisms. Both migraine and cluster headache are widely recognized as brain disorders involving the activation of different cortical, diencephalic, and

brainstem regions and the subsequent release of key neuropeptides, such as the calcitonin gene-related peptide (CGRP).[2] Recent work suggests that the brainstem and hypothalamus might be putative drivers of migraine and cluster headache attacks.[4] Advanced magnetic resonance imaging (MRI) techniques have been applied to the study of migraine and cluster headache patients, both in the course of an acute attack and during the interictal phase, revealing widespread structural and functional abnormalities in brain areas involved in multisensory processing, including pain.[5] Only a few MRI studies[6–8] have directly compared migraine and cluster headache patients, showing bilateral enlargement of the hypothalamus, reduced gray matter (GM) volume of frontal and occipital areas, and increased functional activity of brain cognitive networks in cluster headache patients compared to migraine.

Machine learning techniques provide biomarkers for diagnosis, prognosis, and personalized treatments and shed light on disease pathophysiology. One of the main advantages of using machine learning approaches is that they allow inference at the single-subject level, and they are sensitive to subtle and spatially distributed brain differences that might be undetectable in group-level comparisons.[9] Supervised and unsupervised algorithms of machine learning have been applied to clinical and MRI data to identify distinct phenotypes of migraine, to predict migraine attack onset, disease progression, and treatment response, and to discriminate migraine patients from controls, as well as from other chronic pain disorders.[10–12] A recent study provided insight into predictors of treatment response in cluster headache patients using a supervised machine learning model combining clinical and volumetric imaging data.[13] The potential of machine learning techniques in discriminating migraine from cluster headache patients has not been investigated so far.

In this study, we applied a supervised machine learning approach and multimodal MRI modalities to identify interictal MRI biomarkers that differentiate migraine from cluster headache patients and disclose imaging features shared by these two types of primary headaches. Our working hypothesis was that migraine and cluster headache patients might share some structural and functional abnormalities in cortical and subcortical regions involved in the onset of both types of headache attacks and in pain processing. However, different MRI alterations might explain those clinical features that differ between these conditions. A secondary analysis identified the best clinical predictors of migraine and cluster headache diagnosis and investigated whether a more accurate classification of patients could be achieved combining MRI and clinical data.

Subjects and Methods

Subjects

Between April 2017 and March 2018, 60 migraineurs, 45 cluster headache patients, and 30 healthy controls were prospectively screened for eligibility. Patients were recruited consecutively from the population attending the headache clinics at King's College Hospital. The recruitment of patients and controls was also extended to King's College London staff and students through advertising. To measuring imaging changes related to migraine and cluster headache interictal phase, all brain MRI was performed in a headache-free phase. Moreover, cluster headache patients had to be in the "out of bout" phase to be included, which is when their brain is less prone to have headache attacks. Eligible patients had to meet the following inclusion criteria: (1) diagnosis of an episodic headache disorder; (2) no headache at the time of the MRI; and (3) not using pharmacological preventive treatments for migraine or cluster headache, or drugs affecting the central nervous system for at least 1 month before the MRI. Exclusion criteria for headache patients and controls were any other chronic pain syndrome, neurological, psychiatric, or other major systemic conditions, use of painkillers for >8 days per month, use of illicit drugs, and MRI showing any brain pathology. For migraine, only patients with migraine with aura having attacks with and without aura were enrolled in the study. Only controls who had infrequent tension-type headache were included in the study. Based on inclusion and exclusion criteria, 40 migraineurs, 25 cluster headache patients, and 15 controls were excluded due to chronic headache, the presence of headache the day of the MRI, MRI artifacts, concurrent psychiatric conditions, use of illicit drugs, or use of antidepressants or headache preventive treatments (Fig 1).

Clinical Assessment

Before the MRI examination, the clinical history and neurological examination of all participants were obtained. All patients met the criteria of the International Classification of Headache Disorders for the diagnosis of episodic migraine and episodic cluster headache.[14] Both patients and controls were asked to fill in a headache diary to control whether they had any kind of headache on the days preceding and following the MRI visit. The average headache pain intensity was assessed using a numerical rating scale.[15]

Ethical Approval

The local ethical committee on human studies approved the study, and all subjects provided written informed consent prior to study participation, according to the Declaration of Helsinki.

MRI Acquisition

Using a 3.0T scanner (GE Discovery MR750; GE Medical Systems, Milwaukee, WI), the following brain sequences were acquired: (1) fluid-attenuated inversion recovery (FLAIR; repetition time [TR]/echo time [TE] = 8,000/125 milliseconds, inversion time [TI] = 2,000 milliseconds, flip angle [FlA] = 111°, matrix size = 256 × 128, field of view [FOV] = 240 × 240mm^2, 4mm thick, 36 axial slices),
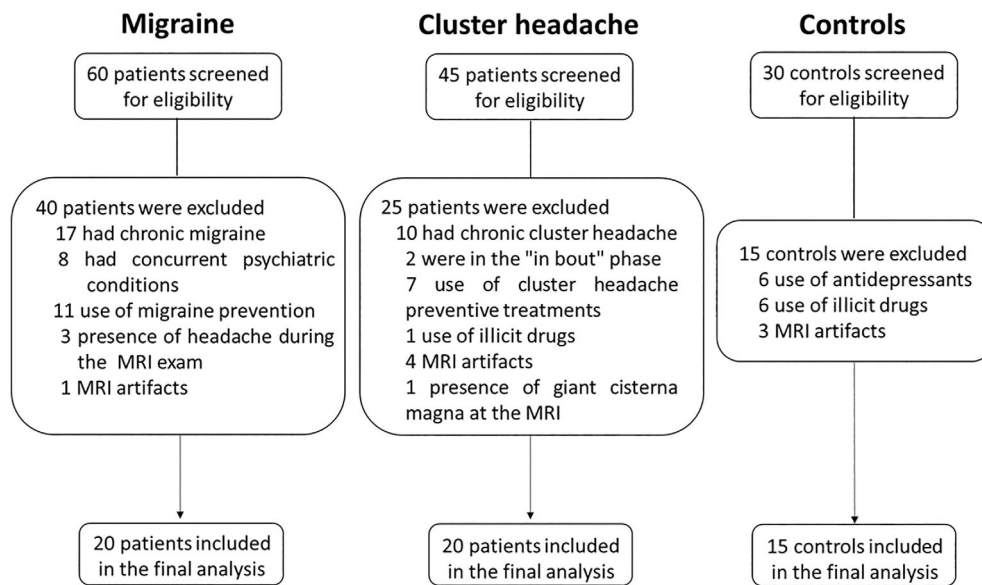
FIGURE 1: A schematic of subjects disposition. MRI = magnetic resonance imaging.

(2) 3-dimensional (3D) T1-weighted gradient echo (TR/TE = 7.3/3.0 milliseconds, TI = 400 milliseconds, FlA = 11°, matrix size = 256 × 256 × 196, FOV = 270 × 270mm^2, 1.2mm thick, 196 sagittal slices), (3) diffusion-weighted (DW) spin-echo (TE/TR = 74/11,250-milliseconds, FlA = 90°, matrix size = 128 × 128, FOV = 256 × 256mm^2, 2mm thick, 72 axial slices, b value = 1,500mm^2/s, DW directions = 60), (4) resting state (RS) functional MRI (fMRI) (TR/TE = 2,500/44 milliseconds, FlA = 80°, matrix size = 64 × 64, FOV = 240 × 240mm^2, 3mm thick, 32 axial slices), and (5) 3D pseudocontinuous arterial spin labeling (pCASL; TE/TR = 11/5,180 milliseconds, FOV = 240 × 240mm^2, 56 slice partitions of 3mm thickness).[16] During fMRI, participants were instructed to keep eyes open. Participants were asked to abstain from taking nonsteroidal anti-inflammatory drugs or paracetamol, having alcohol or caffeine-containing products, and using tobacco- or nicotine-containing products the day before the MRI.

MRI Data Analysis

The presence of white matter (WM) hyperintensities was assessed on FLAIR, and the volume was measured using a local thresholding segmentation technique (Jim 8; Xinapse Systems, West Bergholt, UK).

All images were preprocessed and analyzed to obtain brain volumetric, WM fractional anisotropy (FA), WM mean diffusivity (MD), cerebral blood flow (CBF), and RS functional connectivity (FC) maps (Fig 2A). T1-weighted images were corrected for the presence of WM hyperintensities, then tissue segmentation was performed using the Geodesic Information Flows, generating 3D maps of GM and WM.[17] Afterward, T1 images were nonlinearly registered to the MNI template and the obtained Jacobian volumetric maps of deformation were further masked and used for independent component analysis (ICA).

Diffusion tensor imaging (DTI) data were visually inspected to exclude those having corrupted images. DTI data were preprocessed using ExploreDTI[18] software and corrected for eddy current, motion artifacts and echo-planar imaging geometric distortion. FA and MD maps were then calculated from the diffusion tensor.

The pCASL image was acquired twice to increase statistical power. The two pCASL scans were coregistered and realigned to the T1 space. T1-weighted and proton density images were realigned. CBF maps were skull-stripped and spatially normalized to the MNI standard space. A mean CBF map was obtained from the two preprocessed CBF maps. Finally, CBF maps were spatially smoothed using an 8mm Gaussian kernel.

RS fMRI preprocessing included volume realignment, time series despiking, and slice time correction. After the preprocessing, functional data were optimally combined and denoised with the Multi-Echo ICA approach.[19,20] Then, data were spatially smoothed with an 8mm Gaussian kernel, WM and cerebrospinal fluid signals were regressed out using the maps from the T1 segmentation processing step, a high-pass temporal filter with a cutoff frequency of 0.005Hz was applied, and images were registered to standard MNI152 space.

RS fMRI analysis was focused on subcortical brain areas playing a pivotal role in migraine and cluster headache pathophysiology, including the hypothalamus, dorsal pons, spinal trigeminal nucleus (STN), thalamus, and periaqueductal gray (PAG).[5] A dual regression analysis[21] was used to study voxelwise FC within different regions of interested (ROIs). Based on previous studies, we used a 6mm sphere around the peak MNI coordinates of the hypothalamus (x = ±6, y = −6, z = −10 from Maniyar et al[22] and Schulte et al[23]), and a 3mm sphere around the peak MNI coordinates of the dorsal pons (x = ±6, y = −36, z = −27 from Maniyar et al[22]), STN (x = ±3, y = −36, z = −45 from Stankewitz et ak[24]), and PAG (x = ±6, y = −30, z = −9 from Schwedt et al[25] and Maniyar et al[26]). A thalamic ROI was also defined using the Harvard–Oxford probabilistic anatomical atlas within FSL (thresholded at >20%).

Brain volumetric, WM FA, WM MD, CBF, and RS FC maps of each subject were temporally concatenated using FSL and analyzed using MELODIC group temporal concatenation

ICA[27] (see Fig 2B, C). The ICA outputs are spatial component maps, showing patterns of MRI metric changes across subjects. Each independent component (IC) spatial map was transformed
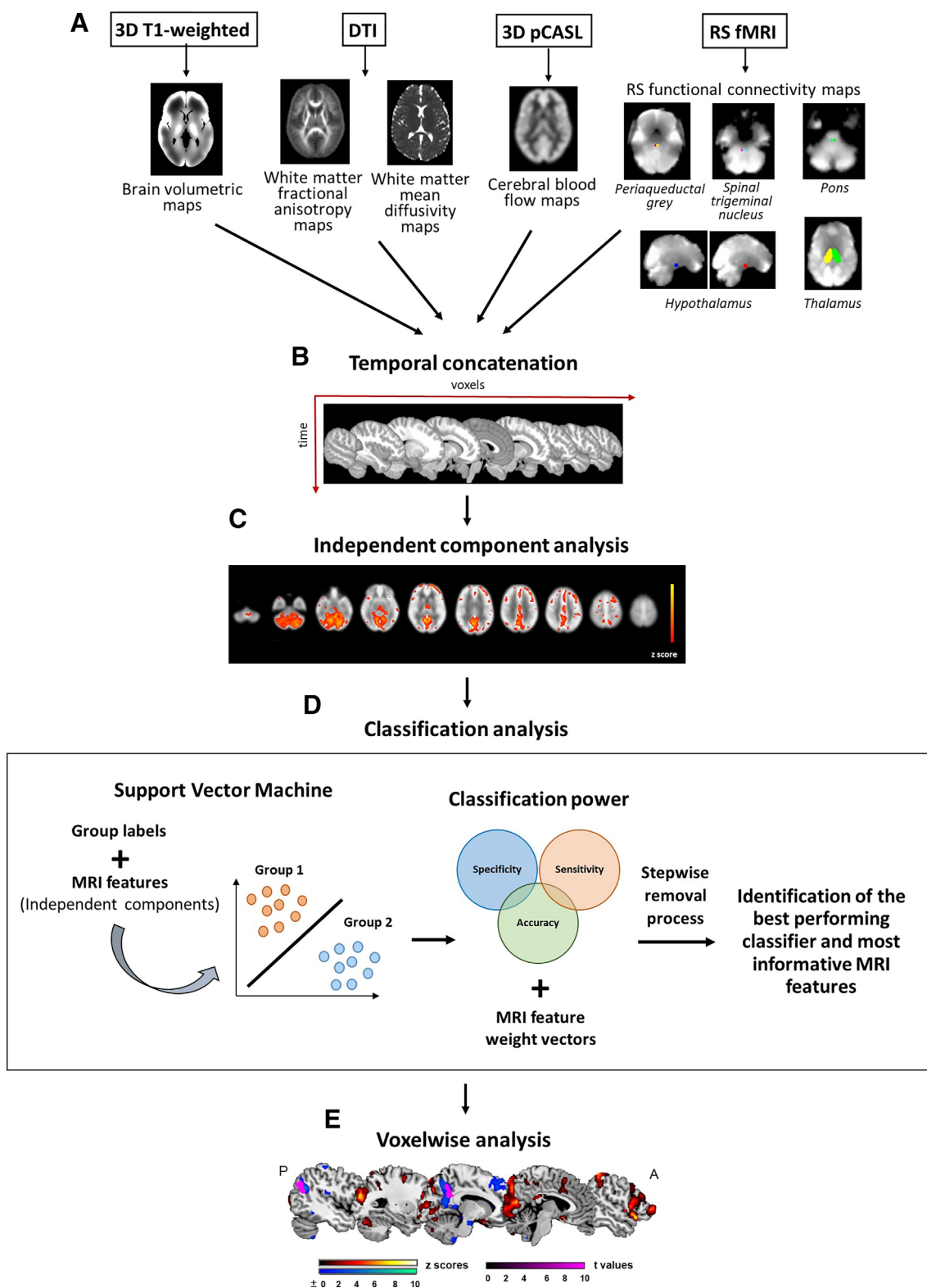
(Figure legend continues on next page.)

to a thresholded voxelwise Z statistics map to infer voxels that were significantly modulated by each subject's contribution.[28] This approach allowed us to transform the original MRI data into a set of features that could be included in the following classification analysis. Five ICs were obtained for each MRI modality. Only those components showing patterns of temporally coherent signal confined to the brain parenchyma were used as features to classify the different groups of participants (see Fig 2C).[29]

Classification Analysis

A linear kernel support vector machine (SVM) model, implemented in the LIBSVM library, was used to assess the most accurate classification of patients and controls. The relative importance of each feature in classifying patients and controls, as well as subgroups of patients, was ranked based on the weight vector provided by the model. After each round of SVM training, the least informative metric was removed and a new SVM trained with the remaining metrics. This process was repeated until only a single feature remained. The accuracy of the classifier was recorded at each stepwise removal. The classifier with the highest accuracy was considered the best performing.[30] Sensitivity and specificity were estimated based on true positives, true negatives, false positives, and false negatives provided by the classification model. Features whose weight vector lay >1 standard deviation (SD) above that of the next highest metric were considered to have the highest importance in the classification.[30] In addition, a 10-fold cross-validation model was performed to assess the generalizability of the results to new subjects. During the cross-validation, the dataset is divided into n folds ($n = 10$ in this case). Then, the model is trained on $n − 1$ folds and its performance is validated on the remaining fold.[31]

First, to investigate which MRI metrics produce the best discrimination of patients and controls and subgroups of patients, we performed a classification analysis including the MRI features obtained from the ICA, which encoded the patterns of brain activation (RS FC and CBF maps) and morphometry (brain volumetric, WM FA, and MD maps; see Fig 2D). Estimation of the classification accuracy was adjusted for age and gender effects. Second, to test the accuracy of clinical features currently used in the diagnosis of migraine and cluster headache, we ran a secondary classification analysis including those clinical characteristics that are considered relatively specific for migraine (photophobia, phonophobia, nausea/vomiting, movement sensitivity, severity and laterality of pain) and cluster headache (CAS, a sense of restlessness, severity and laterality of pain).[14] Age, gender, disease duration, and headache attack frequency were also included in the clinical classification analysis. At last, to investigate whether combined MRI and clinical data would be more accurate in classifying migraine and cluster headache patients, we performed a classification analysis including the MRI and clinical features of the best classification models.

Statistical Analysis

Demographic and clinical characteristics were compared between groups using the Mann–Whitney test for continuous variables and the chi-squared or Fisher exact test for categorical variables (SPSS software, version 22.0; IBM, Armonk, NY).

A total of 500 random permutations were calculated to create the null distribution for assessing the test statistics of the dual regression analyses[21] during the RS fMRI preprocessing. For the ICA, results were thresholded at a $p > 0.5$ level under an alternative hypothesis test based on a Gaussian/gamma mixture model fitted to the intensity histogram of the component.[32]

To establish whether the observed classification accuracy was statistically significant, a repeated random subsampling validation, with a random selection of n subjects removed from both the patient and control group, repeated 1,000 times for each n from 1 to 10, was performed. The association between MRI features with the highest contribution in the classification model and patients' clinical characteristics (side of pain, pain severity, headache attack frequency, disease duration, presence of a sense of restlessness, photophobia, phonophobia, nausea/vomiting, movement sensitivity) was assessed using partial correlation analysis (SPSS software, version 22.0).

Voxelwise t tests were performed to investigate regional between-group differences within the most discriminative MRI features, using SPM12 and a statistical threshold of $p < 0.05$, familywise error-corrected (see Fig 2E). The correlations between such regional differences and patients' clinical features (side of pain, pain severity, headache attack frequency, disease duration, presence of a sense of restlessness, photophobia, phonophobia, nausea/vomiting, movement sensitivity) were assessed using multiple linear regression models as implemented in SPM12. Age and sex were included as covariates in all regional analyses.

FIGURE 2: Overview of magnetic resonance imaging (MRI) data analysis. (A) Images were preprocessed and analyzed to obtain brain volumetric, white matter (WM) fractional anisotropy (FA), WM mean diffusivity (MD), cerebral blood flow (CBF), and resting state (RS) functional connectivity (FC) maps of each subject. (B) Brain volumetric, WM FA, WM MD, CBF, and RS FC maps of each subject were temporally concatenated. (C) An independent component analysis was performed to obtain spatial component maps, showing patterns of covariant MRI metric changes across subjects. Five independent components were obtained for each MRI modality and included in the following classification analysis as MRI features. (D) A support vector machine (SVM) model was used to identify the best performing classifier and most informative MRI features in discrimination of patients and controls, as well as subgroups of patients. The accuracy, sensitivity, and specificity of the model were estimated, and the relative importance of each feature in classifying patients and controls was ranked based on the weight vector provided by the classification model. After each round of SVM training, the least informative metric was removed and a new SVM trained with the remaining metrics. The accuracy of the classifier was recorded at each step of removal. (E) Voxelwise t tests were performed to investigate regional between-group differences within the most discriminative MRI features. 3D = 3-dimensional; A = anterior; DTI = diffusion tensor imaging; fMRI = functional MRI; P = posterior; pCASL = pseudocontinuous arterial spin labeling.

Results

Demographic, Clinical, and Conventional MRI Data

A total of 20 migraineurs (10 without and 10 with aura), 20 cluster headache patients, and 15 controls were included in the final analysis. A migraine patient reported a migraine attack the day before the MRI, whereas all other patients were headache-free for at least 2 days before the examination. Most of the migraine patients also denied having headaches in the days following the MRI (data not available for 5 patients). All cluster headache patients were scanned when they were out of bout and none of them had any headache attacks for at least 48 hours before and after the MRI. Beyond cluster headache, 3 patients had also migraine without aura attacks (Patient 1: 2 attacks in 6 years; Patient 2: 4 attacks per year; Patient 3: 4 attacks per month), 2 patients used to suffer from migraine without aura during their adolescence, and 4 patients also had a diagnosis of probable migraine. Eight controls suffered from infrequent tension type headache. None of the controls reported any headaches before or after the MRI.

Headache patients were older than controls, whereas gender did not differ between headache patients and controls (Table 1). Compared to controls and migraine patients, cluster headache patients were the oldest, whereas age did not differ between migraineurs and controls. As expected, considering the gender prevalence of the two diseases, migraine patients were predominantly females, whereas most of the cluster headache patients were males. The median number of headache attacks per month in migraineurs was 4 (interquartile range [IQR] = 2–56). Cluster headache patients had a median of 0.8 bouts per year (IQR = 0.5–1), lasting a median of 45 days (IQR = 30–71), and 3 attacks per day (IQR = 1–3). Photophobia, phonophobia, movement sensitivity, and nausea/vomiting were more prevalent in migraine patients, whereas a sense of restlessness and unilateral pain were more frequent in cluster headache patients. Compared to migraine patients, patients with cluster headache experienced more severe headache attacks.

Two migraine, 4 cluster headache, and 2 control subjects had small, nonspecific, punctate WM hyperintensities, with no significant between-group differences in the mean lesion volume (see Table 1).

Feature Selection

Different structural and fMRI patterns, including the brainstem, cerebellum, thalamus, basal ganglia, and frontal, parietal, temporal, and occipital areas, were selected from the ICA and included as features in the MRI classification analyses. Clinical and demographic features included in the clinical classification analysis were age, sex, disease duration, headache attack frequency, presence of photophobia, phonophobia, nausea/vomiting, movement sensitivity, CAS, and restlessness, and severity and laterality of pain.

Classification Analysis

Headache Patients and Controls. The MRI model yielding the highest classification accuracy in discriminating controls from headache patients achieved an accuracy of 80% ($p = 0.006$; Fig 3 and Table 2). Although there were no MRI features whose weight vector exceeded 1 SD of the next highest metric, the right hypothalamic RS FC IC3, left hypothalamic RS FC IC5, and left RS FC IC4 of the PAG had the highest feature importance in the prediction. In the RS FC IC3, the right hypothalamus had an increased FC with the insular, parietal, occipital, and temporal areas. In contrast, the left hypothalamus showed decreased FC with the insular, parietal, occipital, and temporal areas in the RS FC IC5. In the RS FC IC4, the left PAG had a decreased RS FC with the pons, and medial and superior frontal gyrus, as well as an increased RS FC with the precuneus, occipital areas, and middle temporal and orbitofrontal gyrus. We found a positive correlation between the RS FC IC4 of the left PAG and the presence of movement sensitivity ($r = 0.4$, $p = 0.009$), phonophobia ($r = 0.3$, $p = 0.05$), and nausea/vomiting ($r = 0.3$, $p = 0.03$). The RS FC IC4 of the left PAG was negatively correlated with the presence of CAS ($r = -0.3$, $p = 0.04$) and pain severity ($r = -0.3$, $p = 0.04$).

Migraine Patients and Controls. The best MRI classifier in discriminating migraineurs and controls yielded an accuracy of 89% ($p = 0.008$; Fig 4A and Table 2). The RS FC IC4 of the right PAG had the highest feature importance in the classification. In this RS network, the right PAG had an increased RS FC with frontal areas and the insula, and a decreased RS FC with the cerebellum, and inferior occipital and orbitofrontal gyrus (see Fig 4C). In migraine patients, a positive correlation was observed between the RS FC IC4 of the right PAG and the presence of CAS ($r = 0.5$, $p = 0.02$).

Cluster Headache Patients and Controls. The MRI model with the best performance in distinguishing cluster headache patients from controls had an accuracy of 98% ($p < 0.001$; see Fig 4B and Table 2). The right RS FC IC4 of the PAG was the MRI feature with the highest importance in the prediction. No significant correlations were found between the RS FC IC4 of the right PAG and cluster headache patients' clinical characteristics.

TABLE 1. Demographic, Clinical, and Conventional Magnetic Resonance Imaging Characteristics of Controls and Patients

| Characteristic	Controls	Headache Patients	Migraine	Cluster Headache	Headache vs Controls, p	Migraine vs Controls, p	Cluster Headache vs Controls, p	Migraine vs Cluster Headache, p
Women/men	8/7	22/18	18/2	4/16	0.6	0.02	0.07	<0.001
Age, yr	24 (23–28)	34 (27–45)	29 (24–31)	41 (26–56)	<0.001	0.07	<0.001	<0.001
Disease duration, yr	—	15 (9–21)	14 (8–17)	16 (10–25)	—	—	—	0.2
Headache attack frequency per year	—	51 (20–89)	45 (18–68)	68 (32–127)	—	—	—	0.06
Presence of								
Movement sensitivity	—	23	20	3	—	—	—	<0.001
Photophobia	—	28	19	9	—	—	—	0.001
Phonophobia	—	23	17	6	—	—	—	0.001
Nausea/vomiting	—	31	19	12	—	—	—	0.02
Cranial autonomic symptoms	—	37	17	20	—	—	—	0.2
Restlessness	—	23	3	20	—	—	—	<0.001
Unilateral pain	—	29	9	20	—	—	—	<0.001
Right		14	1	13				
Left		7	2	5				
Right or left		8	6	2				
NRS score	—	8.5 (7.1–10)	7.2 (6.6–8.4)	10 (8.6–10)	—	—	—	<0.001
Mean WMH lesion volume ± standard deviation, ml	0.027 ± 0.08	0.088 ± 0.32	0.054 ± 0.23	0.122 ± 0.39	0.9	0.8	0.6	0.4

Note: Measures are reported as median and interquartile range (25th–75th percentiles). Gender and patients' clinical features are reported as frequencies.

Abbreviation: NRS = numerical rating scale; WMH = white matter hyperintensity.

Migraine and Cluster Headache Patients. The MRI model yielding the highest classification accuracy in discriminating cluster headache from migraine patients achieved an accuracy of 78% ($p = 0.01$; Fig 5A and Table 2). The left thalamic RS FC IC4 had the highest feature importance in the classification. In this network, the left thalamus showed a decreased RS FC with parietal regions, middle temporal and medial frontal gyrus, and an increased RS FC with the cerebellum, cingulum, middle frontal gyrus, and occipital areas (see Fig 5B). We did not find any significant association between the left thalamic RS FC IC4 and patients' clinical features.

The best classification accuracy for correctly classifying individual patients as having migraine or cluster headache based on all demographic and clinical features was 99% ($p < 0.001$; see Fig 5C and Table 2). Although there were no clinical features whose weight vector exceeded 1 SD of the next highest metric, the presence of restlessness and the severity of pain had the highest feature importance in the prediction.

The best MRI–clinical combined classification model achieved an accuracy of 99% ($p < 0.001$; see Fig 5D and Table 2). The presence of restlessness was the feature with the highest importance in the prediction.
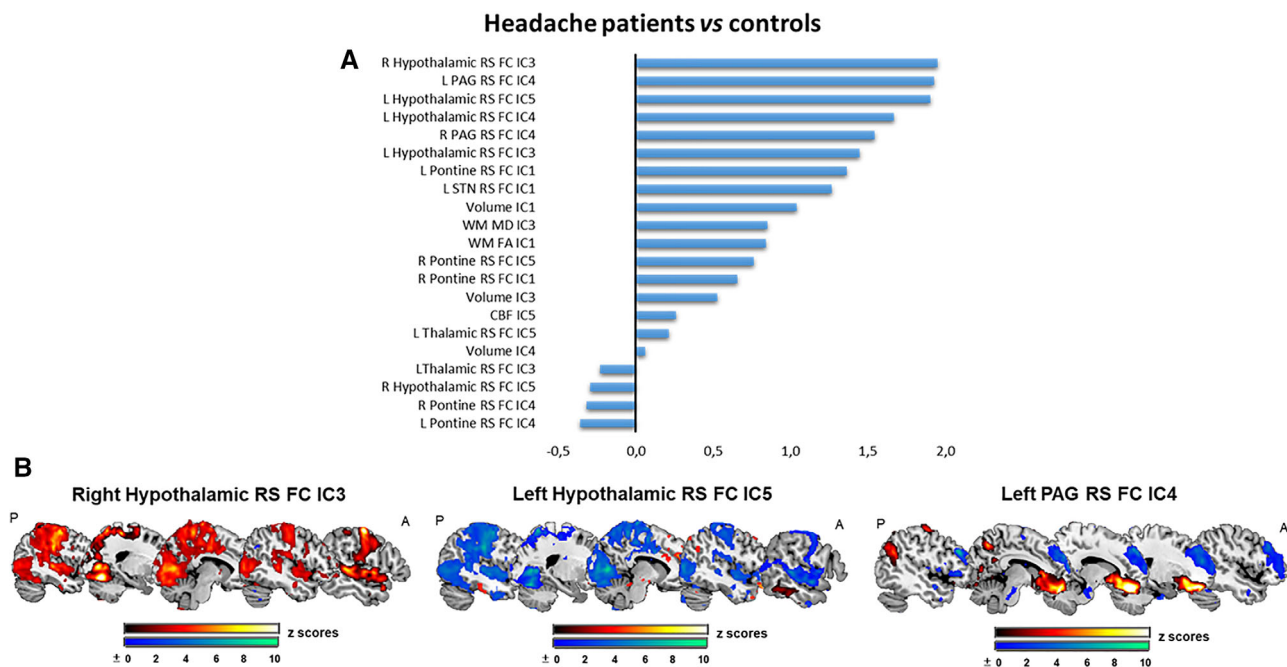
FIGURE 3: Classification model discriminating headache patients from controls. (A) The bar graph represents normalized weights of magnetic resonance imaging (MRI) features included in the model yielding the highest classification accuracy in discriminating controls from the entire group of headache patients. (B) Spatial maps of the MRI features with the highest importance in the prediction. Maps were thresholded at a $p > 0.5$ level under an alternative hypothesis. High z scores are represented in red-yellow and low z scores are represented in blue. A = anterior; CBF = cerebral blood flow; FA = fractional anisotropy; FC = functional connectivity; IC = independent component; L = left; MD = mean diffusivity; P = posterior; PAG = periaqueductal gray; R = right; RS = resting state; STN = spinal trigeminal nucleus; WM = white matter.

TABLE 2. Classification Performance of the Most Discriminative Models Differentiating Headache Patients from Controls, as Well as Migraine from Cluster Headache Patients

MRI Classifier Performance

Headache vs Controls			Migraine vs Controls			Cluster Headache vs Controls		
Accuracy, %	Sensitivity, %	Specificity, %	Accuracy, %	Sensitivity, %	Specificity, %	Accuracy, %	Sensitivity, %	Specificity, %
80	87	66	89	95	80	98	80	100
	Headache	Controls		Migraine	Controls		Cluster headache	Controls
Headache	35	5	Migraine	19	1	Cluster headache	16	4
Controls	5	10	Controls	3	12	Controls	0	15

Migraine vs Cluster Headache

MRI Classifier Performance			Clinical Classifier Performance			MRI–Clinical Combined Classifier Performance		
Accuracy, %	Sensitivity, %	Specificity, %	Accuracy, %	Sensitivity, %	Specificity, %	Accuracy, %	Sensitivity, %	Specificity, %
78	65	70	99	95	100	99	95	100
	Migraine	Cluster headache		Migraine	Cluster headache		Migraine	Cluster headache
Migraine	13	7	Migraine	19	1	Migraine	19	1
Cluster headache	6	14	Cluster headache	0	20	Cluster headache	0	20

Abbreviation: MRI = magnetic resonance imaging.
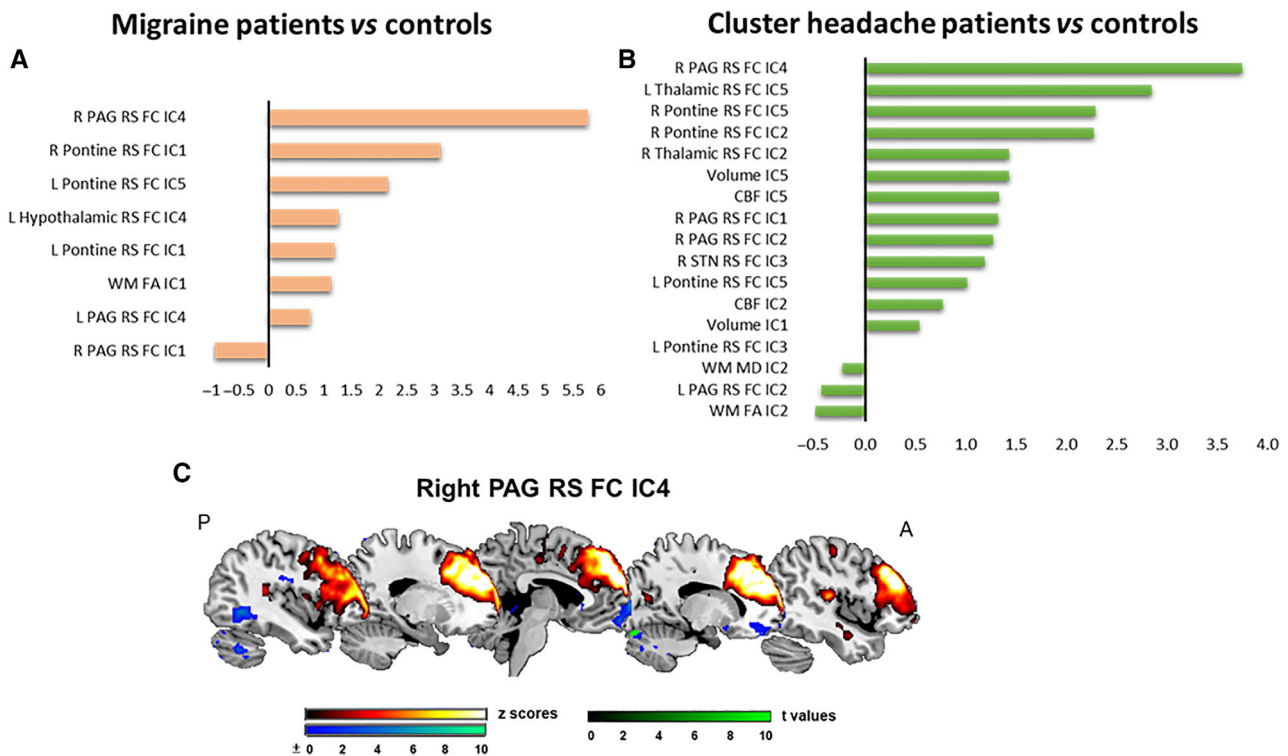
FIGURE 4: Classification model discriminating migraine patients and cluster headache patients from controls. (A) The bar graph represents normalized weights of magnetic resonance imaging (MRI) features included in the model yielding the highest classification accuracy in discriminating migraine patients from controls. (B) The bar graph represents normalized weights of MRI features included in the model yielding the highest classification accuracy in discriminating cluster headache patients from controls. (C) Spatial map of the resting state (RS) functional connectivity (FC) independent component 4 (IC4) of the right periaqueductal gray (PAG) thresholded at a $p > 0.5$ level under an alternative hypothesis. High z scores are represented in red–yellow and low z scores are represented in blue. Brain regions showing increased RS FC with the right PAG in migraine patients compared to controls are shown in green (color-coded for their t values; $p < 0.05$, clusterwise familywise error-corrected for multiple comparisons). A = anterior; CBF = cerebral blood flow; FA = fractional anisotropy; L = left; MD = mean diffusivity; P = posterior; R = right; STN = spinal trigeminal nucleus; WM = white matter.

Voxelwise Analyses

There were no significant brain regional differences between headache patients and controls in the left hypothalamic RS FC IC5, right hypothalamic RS FC IC3, and the RS FC IC4 of the left PAG, as well as between cluster headache patients and controls in the RS FC IC4 of the right PAG.

Within the RS FC IC4 of the right PAG, an increased RS FC between the right PAG and ipsilateral cerebellum was found in migraine patients compared to controls (see Fig 4C and Table 3).

Within the left thalamic RS FC IC4, compared to migraine patients, cluster headache patients showed decreased RS FC between the left thalamus and left precuneus, and angular and middle temporal gyrus (see Fig 4B and Table 3).

No significant correlations were found between such functional alterations and migraine patients' clinical characteristics.

Discussion

In this study, using a supervised machine learning approach and multimodal imaging data, we identified the most discriminative MRI patterns that distinguish migraine from cluster headache patients, as well as imaging features shared by these two primary headaches.

Our results showed a robust and accurate classification of patients with primary headaches and controls, achieving an accuracy of 80%. When we trained the model to discriminate migraine and cluster headache patients from controls separately, an overall accuracy of 89% and 98%, respectively, was obtained.

The first interesting result of our study is that the combination of different patterns of brain activation and morphometry yielded the best classification performance in distinguishing migraine and cluster headache patients from controls. Previously, a lower accuracy rate ranging from 67% to 86% was obtained for distinguishing migraine patients from controls.[33,34] These results were obtained by supervised classification algorithms including only brain cortical morphometric measures or RS FC data. Previous MRI studies using classification or univariate standard approaches have separately investigated structural and functional imaging features, showing abnormalities in

Migraine *vs* cluster headache patients
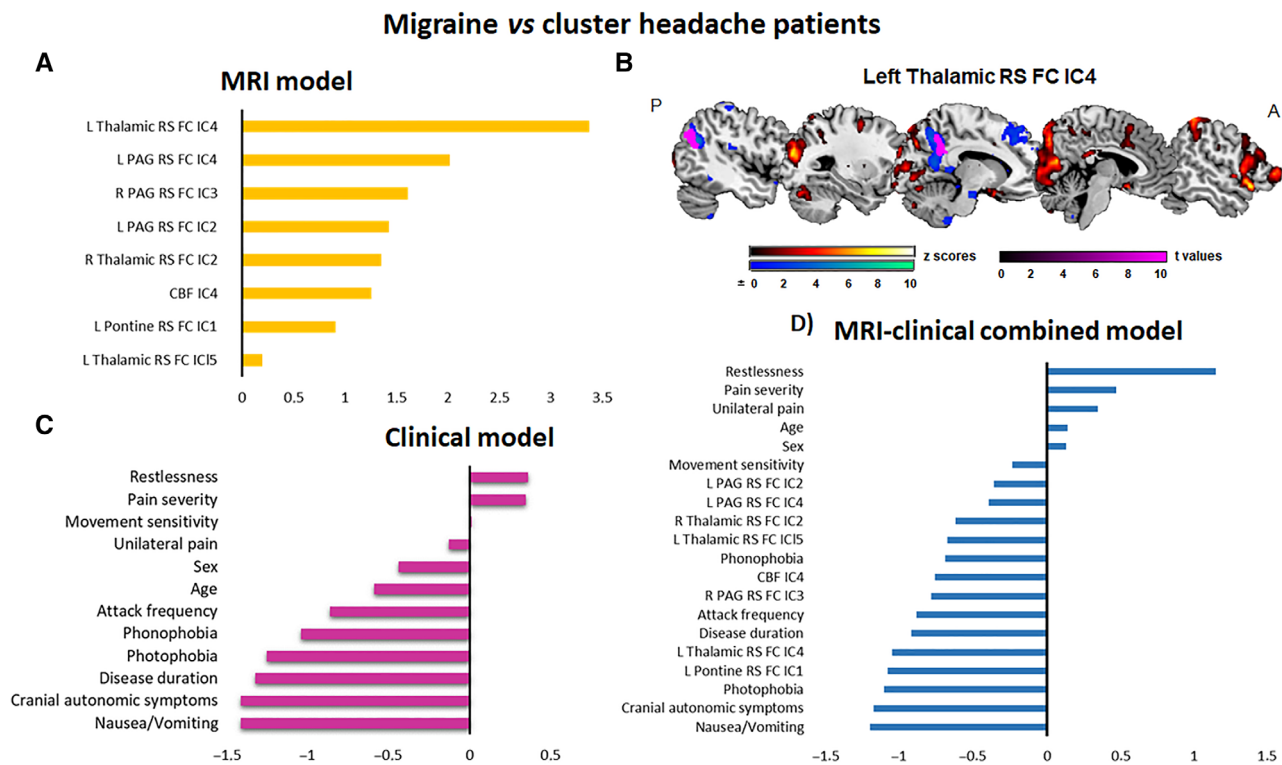
FIGURE 5: Classification models discriminating migraine from cluster headache patients. (A) The bar graph represents normalized weights of magnetic resonance imaging (MRI) features included in the model yielding the highest classification accuracy in discriminating migraine from cluster headache patients. (B) Spatial map of the resting state (RS) functional connectivity (FC) independent component 4 (IC4) of the left thalamus thresholded at a *p* > 0.5 level under an alternative hypothesis. High *z* scores are represented in red–yellow and low *z* scores are represented in blue. Brain regions showing decreased RS FC with the left thalamus in cluster headache patients compared to migraine patients are shown in violet (color-coded for their *t* values; *p* < 0.05, clusterwise familywise error-corrected for multiple comparisons). (C) The bar graph represents normalized weights of clinical and demographic features included in the clinical model yielding the highest classification accuracy in discriminating migraine from cluster headache patients. (D) The bar graph represents normalized weights of clinical, demographic, and MRI features included in the MRI–clinical combined model yielding the highest classification accuracy in discriminating migraine from cluster headache patients. A = anterior; CBF = cerebral blood flow; L = left; P = posterior; PAG = periaqueductal gray; R = right.

TABLE 3. Regional Resting State Functional Connectivity Differences between Migraine Patients and Controls, as Well as between Cluster Headache and Migraine Patients

Migraine vs Controls

Cerebral Regions Showing Increased RS FC with the Right PAG in Migraine Patients	Brodmann Area	*t* Values[a]	Cluster Extent (no. of voxels)	MNI Coordinates, x, y, z
Right cerebellum (crus I)	—	6.04	655	−9, −85, −19

Migraine vs Cluster Headache

Cerebral Regions Showing Decreased RS FC with the Left Thalamus in Cluster Headache Patients	Brodmann Area	*t* Values[a]	Cluster Extent (no. of voxels)	MNI Coordinates, x, y, z
Left angular gyrus	39	4.90	662	−46, −72, 32
Left middle temple gyrus	39	4.24		−48, −63, 20
Left precuneus	7	4.08	457	−10, −55, 44

[a]*p* < 0.05, clusterwise familywise error-corrected for multiple comparisons.

Abbreviation: FC = functional connectivity; MNI = Montreal Neurological Institute; PAG = periaqueductal gray; RS = resting state.

brain areas involved in multisensory processing, including pain, in both migraine and cluster headache patients.[5] Only one previous classification study demonstrated the advantage of combining GM volume and RS fMRI data over the single imaging feature in the discrimination between migraineurs and controls (83% vs 71% of accuracy).[35] Moreover, only a few studies using standard univariate analysis have explored the presence of concurrent GM volume and functional brain changes in migraine patients.[36,37] In this study, volumetric and RS fMRI measures have been integrated with DTI and pCASL data, providing comprehensive information regarding hemodynamic, functional, macrostructural, and microstructural changes of the brain. The integration of multiple functional and structural imaging metrics discloses complementary information regarding the underlying biological processes. This approach might help us to achieve a better understanding of headache pathophysiology.

Supervised classification algorithms have never been used, so far, to distinguish cluster headache patients from controls. Interestingly, we found a classification accuracy for discrimination between cluster headache and controls of 98%, with a specificity of 100%. These results suggest that being sure a control does not harbor cluster headache biology is not as challenging as for migraine.[2]

The most discriminative MRI patterns in classifying migraine and cluster headache patients from controls included brain RS FC networks of the PAG and hypothalamus. The prominent role of the hypothalamus in migraine and cluster headache pathophysiology is well established. There is ample evidence supporting a key role of the hypothalamus in the acute phase of migraine and cluster headache attacks.[22,38,39] Recent fMRI studies during trigeminal nociceptive stimulation highlighted dynamic functional changes of hypothalamic activity during the migraine and cluster headache cycle, supporting its pivotal involvement in driving the onset of headache attacks.[40,41] Similar to previous interictal studies,[7,42,43] here we showed a significant functional interaction between the hypothalamus and brain areas implicated in pain control and visual processing in both migraine and cluster headache patients studied outside their headache attacks. Our findings are also in line with a previous classification study reporting that the RS FC between the amygdala and hypothalamus contributed to the classification accuracy of distinguishing migraine patients from controls.[31]

The PAG is a key area of the endogenous pain inhibitory system.[44] There is evidence revealing an altered functional interaction between nociceptive brain areas and the PAG that might contribute to the development of allodynia in migraine patients.[25] It has also been shown that PAG stimulation could provoke the onset of headache pain.[45,46] Here, we have found a specific involvement of the networks connecting the left and right PAG to the cerebellum, insula, and frontal, temporal, and occipital areas in the whole group of headache patients, as well as in migraine and cluster headache patients separately. Although the role of the RS FC of the PAG in headache classification has not been investigated so far, previous studies confirmed the involvement of pain-processing brain areas, comprising the insular, cerebellar, temporal, and frontal regions, in discriminating migraine patients from controls.[33–35] It is worth noting that although the left and right PAG were connected with similar brain areas, they showed an opposite direction of their functional coupling. The significant association we have found in headache patients between the left RS FC network of the PAG and pain severity reinforce its crucial role in modulating pain perception. Interestingly, in our sample of patients the global functional activity of the PAG networks was also significantly associated with the presence of CAS and migraine-specific symptomatology, like movement sensitivity, phonophobia, and nausea/vomiting. These findings are in line with a previous positron emission tomography study[26] suggesting a possible contribution of the PAG to the presence of nausea in migraine patients and preclinical studies showing an involvement of the PAG in the control of sensory, autonomic, and motor processes.[47] PAG activity can be modulated by various neuropeptides and neurotransmitters involved in migraine and cluster headache pathophysiology, such as serotonin, orexin, and CGRP, suggesting the PAG as a possible site of action of acute and preventive headache treatments, like triptans and anti-CGRP monoclonal antibodies.[47,48] Our findings highlighted the PAG as one of the mediators of symptoms accompanying migraine and cluster headache pain, supporting its containing potential therapeutic targets.

The MRI model discriminating cluster headache and migraine patients achieved the lowest accuracy rate (78%). Interestingly, beyond cluster headache attacks, 9 patients had also a history of definite or probable migraine without aura. These data are in line with previous findings demonstrating a higher prevalence of migraine and family history of migraine in cluster headache patients.[49] The coexistence of the two types of headaches in 45% of cluster headache patients might explain the lower accuracy rate we obtained and support common genetic predisposition and pathophysiological mechanisms between migraine and cluster headache. We cannot exclude that the inclusion of cluster headache patients studied during the "in bout" phase may increase the accuracy rate. There is evidence showing dynamic functional and structural brain changes in cluster headache patients between the "in bout" and "out of bout" phases of the disease, suggesting that these changes may facilitate the onset of cluster headache attacks.[3] The study of cluster headache patients during the most active phase of their disease may unveil more imaging differences

in comparison to migraine patients. Adding patients' clinical features to the MRI measures improved the classification accuracy of the model distinguishing migraine from cluster headache patients, reaching an overall accuracy of 99%. Clinical characteristics of patients provided the highest accuracy in identifying individuals as having migraine or cluster headache, thus reinforcing the importance of clinical criteria for the differential diagnosis of these two forms of primary headaches. Interestingly, both clinical and MRI–clinical combined models revealed that the most important feature in discriminating migraine and cluster headache patients was the presence of restlessness. Behavioral disturbances, such as restlessness and agitation, are relatively cluster headache-specific symptoms often described by patients.[3] In our sample, all patients with cluster headache reported the experience of restlessness during their attacks.

The identification of the most discriminative MRI features revealed a central role of the thalamus in classifying migraine from cluster headache patients. We found a lower functional interaction between the left thalamus and parietal brain regions, including the precuneus and angular gyrus, in cluster headache compared to migraine patients. The thalamus is a key area for the processing and integration of nociceptive stimuli. Thalamocortical projections to somatosensory, motor, visual, and limbic regions can explain part of the complexity of headache features.[50] The precuneus and angular gyrus are components of the default mode network, a brain network known to be involved in cognition, self-monitoring, sensory integration, and interoception.[51] Based on our results, we could speculate that an abnormal processing of the inner-generated sensory stimuli may lead to the sense of agitation and the compulsion to move described by patients with cluster headache. This hypothesis is in line with previous evidence showing an association between abnormal thalamocortical activity and the presence of agitation in patients with restless leg syndrome or psychiatric disorders.[52,53]

The main strengths of this study are the integration of multimodal functional and structural MRI data and combination of imaging and clinical data. Moreover, for the first time, we have used supervised classification algorithms to distinguish cluster headache patients from controls, as well as migraine from cluster headache patients.

Moving to limitations, the study has a relatively small sample size. For this reason, we have decided to use a supervised machine learning approach, which performs biomarkers extraction at the level of each patient independently of sample size.[9] In addition, the sample size of patients and controls is in line with previous MRI studies in headache disorders.[54] Both migraine patients with and without aura were included in the study, and many cluster headache patients had migrainous biology. Participants with both migraine and cluster headache biologies may blur important distinctions. Our results should be validated in an independent sample. Moreover, further studies to classify migraine and cluster headache patients in the ictal and interictal phases are warranted.

Although a detailed clinical history remains the mainstay for migraine and cluster headache diagnosis, our data highlight the potential value of machine learning techniques and multimodal MRI data in understanding the neurobiological basis of migraine and cluster headache. MRI classifiers including brain functional and structural MRI measures accurately classified individuals as having migraine or cluster headache, supporting the view of these primary headaches as complex brain disorders. We identified brain functional biomarkers, including the hypothalamic and PAG networks, shared by migraine and cluster headache, that could mediate the pain and associated symptoms experienced by patients. We also proposed the thalamocortical pathway as the neural substrate that could differentiate migraine from cluster headache attacks with their distinct clinical features. As newer acute and preventive therapies are licensed, the application of machine learning techniques and multimodal MRI data may cast further light on primary headache physiopathology, reveal new therapeutic targets, and guide the development of new drugs tailored to each form of primary headache.

Author Contributions

R.M. and P.J.G. contributed to the conception and design of the study. R.M. and C.H.S. contributed to the acquisition and analysis of data. All authors contributed to drafting the text or preparing the figures.

Potential Conflicts of Interest

Nothing to report.

Data Availability Statement

Data supporting the findings of this study are available from the corresponding author upon reasonable request.

References

1. Diseases GBD, Injuries C. Global burden of 369 diseases and injuries in 204 countries and territories, 1990-2019: a systematic analysis for the global burden of disease study 2019. Lancet 2020;396:1204–1222.

2. Goadsby PJ, Holland PR, Martins-Oliveira M, et al. Pathophysiology of migraine: a disorder of sensory processing. Physiol Rev 2017;97: 553–622.

3. May A, Schwedt TJ, Magis D, et al. Cluster headache. Nature reviews Disease primers 2018;1:18006.

4. Hoffmann J, Baca SM, Akerman S. Neurovascular mechanisms of migraine and cluster headache. J Cereb Blood Flow Metab 2017;1: 271678X17733655.

5. Messina R, Filippi M, Goadsby PJ. Recent advances in headache neuroimaging. Curr Opin Neurol 2018;31:379–385.

6. Arkink EB, Schmitz N, Schoonman GG, et al. The anterior hypothalamus in cluster headache. Cephalalgia 2017;37:1039–1050.

7. Chong CD, Aguilar M, Schwedt TJ. Altered hypothalamic region covariance in migraine and cluster headache: a structural MRI study. Headache 2020;60:553–563.

8. Giorgio A, Lupi C, Zhang J, et al. Changes in grey matter volume and functional connectivity in cluster headache versus migraine. Brain Imaging Behav 2020;14:496–504.

9. Orru G, Pettersson-Yeo W, Marquand AF, et al. Using support vector machine to identify imaging biomarkers of neurological and psychiatric disease: a critical review. Neurosci Biobehav Rev 2012;36:1140–1152.

10. Messina R, Filippi M. What we gain from machine learning studies in headache patients. Front Neurol 2020;11:221.

11. Spaink HAVI, Leeuwen MV, Terwindt GM. Methodological considerations in predicting migraine attacks using machine learning. Cephalalgia 2022;2:10.

12. Gonzalez-Martinez A, Pagan J, Sanz-Garcia A, et al. Machine-learning-based approach for predicting response to anti-calcitonin gene-related peptide (CGRP) receptor or ligand antibody treatment in patients with migraine: a multicenter Spanish study. Eur J Neurol 2022;29:3102–3111.

13. Tso AR, Brudfors M, Danno D, et al. Machine phenotyping of cluster headache and its response to verapamil. Brain 2021;144:655–664.

14. Headache classification Committee of the International Headache S. the international classification of headache disorders, 3rd edition (beta version). Cephalalgia 2013;33:629–808.

15. Lines CR, Vandormael K, Malbecq W. A comparison of visual analog scale and categorical ratings of headache pain in a randomized controlled clinical trial with migraine patients. Pain 2001;93:185–190.

16. Alsop DC, Detre JA, Golay X, et al. Recommended implementation of arterial spin-labeled perfusion MRI for clinical applications: a consensus of the ISMRM perfusion study group and the European consortium for ASL in dementia. Magn Reson Med 2015;73:102–116.

17. Sudre CH, Bocchetta M, Heller C, et al. White matter hyperintensities in progranulin-associated frontotemporal dementia: a longitudinal GENFI study. NeuroImage Clinical 2019;24:102077.

18. Forkel SJ, Thiebaut de Schotten M, Dell'Acqua F, et al. Anatomical predictors of aphasia recovery: a tractography study of bilateral perisylvian language networks. Brain 2014;137:2027–2039.

19. Kundu P, Brenowitz ND, Voon V, et al. Integrated strategy for improving functional connectivity mapping using multiecho fMRI. Proc Natl Acad Sci U S A 2013;110:16187–16192.

20. Posse S, Wiese S, Gembris D, et al. Enhancement of BOLD-contrast sensitivity by single-shot multi-echo functional MR imaging. Magn Reson Med 1999;42:87–97.

21. Smith DV, Utevsky AV, Bland AR, et al. Characterizing individual differences in functional connectivity using dual-regression and seed-based approaches. Neuroimage 2014;15:1–12.

22. Maniyar FH, Sprenger T, Monteith T, et al. Brain activations in the premonitory phase of nitroglycerin-triggered migraine attacks. Brain 2014;137:232–241.

23. Schulte LH, Allers A, May A. Hypothalamus as a mediator of chronic migraine: evidence from high-resolution fMRI. Neurology 2017;88: 2011–2016.

24. Stankewitz A, Aderjan D, Eippert F, May A. Trigeminal nociceptive transmission in migraineurs predicts migraine attacks. J Neurosci 2011;31:1937–1943.

25. Schwedt TJ, Larson-Prior L, Coalson RS, et al. Allodynia and descending pain modulation in migraine: a resting state functional connectivity analysis. Pain Med 2014;15:154–165.

26. Maniyar FH, Sprenger T, Schankin C, Goadsby PJ. The origin of nausea in migraine-a PET study. J Headache Pain 2014;3:84.

27. Beckmann CF, Smith SM. Tensorial extensions of independent component analysis for multisubject FMRI analysis. Neuroimage 2005;25: 294–311.

28. Beckmann CF. Modelling with independent components. Neuroimage 2012;62:891–901.

29. Smith SM, Miller KL, Moeller S, et al. Temporally-independent functional modes of spontaneous brain activity. Proc Natl Acad Sci U S A 2012;109:3131–3136.

30. Fagerholm ED, Hellyer PJ, Scott G, et al. Disconnection of network hubs and cognitive impairment after traumatic brain injury. Brain 2015;138:1696–1709.

31. Doyle OM, Mehta MA, Brammer MJ. The role of machine learning in neuroimaging for drug discovery and development. Psychopharmacology (Berl) 2015;232:4179–4189.

32. Beckmann CF, Smith SM. Probabilistic independent component analysis for functional magnetic resonance imaging. IEEE Trans Med Imaging 2004;23:137–152.

33. Chong CD, Gaw N, Fu Y, et al. Migraine classification using magnetic resonance imaging resting-state functional connectivity data. Cephalalgia 2017;37:828–844.

34. Schwedt TJ, Chong CD, Wu T, et al. Accurate classification of chronic migraine via brain magnetic resonance imaging. Headache 2015;55:762–777.

35. Zhang Q, Wu Q, Zhang J, et al. Discriminative analysis of migraine without Aura: using functional and structural MRI with a multi-feature classification approach. PLoS One 2016;11:e0163875.

36. Mehnert J, May A. Functional and structural alterations in the migraine cerebellum. J Cereb Blood Flow Metab 2017;1: 271678X17722109.

37. Maleki N, Becerra L, Brawn J, et al. Concurrent functional and structural cortical alterations in migraine. Cephalalgia 2012;32:607–620.

38. May A, Bahra A, Buchel C, et al. Hypothalamic activation in cluster headache attacks. Lancet 1998;352:275–278.

39. Denuelle M, Fabre N, Payoux P, et al. Hypothalamic activation in spontaneous migraine attacks. Headache 2007;47:1418–1426.

40. Schulte LH, May A. The migraine generator revisited: continuous scanning of the migraine cycle over 30 days and three spontaneous attacks. Brain 2016;139:1987–1993.

41. Schulte LH, Haji AA, May A. Phase dependent hypothalamic activation following trigeminal input in cluster headache. J Headache Pain 2020;21:30.

42. Messina R, Rocca MA, Valsasina P, et al. Clinical correlates of hypothalamic functional changes in migraine patients. Cephalalgia 2022; 42:279–290.

43. Yang FC, Chou KH, Fuh JL, et al. Altered hypothalamic functional connectivity in cluster headache: a longitudinal resting-state functional MRI study. J Neurol Neurosurg Psychiatry 2015;86:437–445.

44. Mainero C, Boshyan J, Hadjikhani N. Altered functional magnetic resonance imaging resting-state connectivity in periaqueductal gray networks in migraine. Ann Neurol 2011;70:838–845.

45. Raskin NH, Hosobuchi Y, Lamb S. Headache may arise from perturbation of brain. Headache 1987;27:416–420.

46. Leone M. Deep brain stimulation in headache. Lancet Neurol 2006; 5:873–877.

47. Akerman S, Holland PR, Goadsby PJ. Diencephalic and brainstem mechanisms in migraine. Nat Rev Neurosci 2011;12:570–584.

48. Bartsch T, Knight YE, Goadsby PJ. Activation of 5-HT(1B/1D) receptor in the periaqueductal gray inhibits nociception. Ann Neurol 2004;56:371–381.

49. Bahra A, May A, Goadsby PJ. Cluster headache: a prospective clinical study with diagnostic implications. Neurology 2002;58:354–361.

50. Noseda R, Jakubowski M, Kainz V, et al. Cortical projections of functionally identified thalamic trigeminovascular neurons: implications for migraine headache and its associated symptoms. J Neurosci 2011;31:14204–14217.

51. Buckner RL, Andrews-Hanna JR, Schacter DL. The brain's default network: anatomy, function, and relevance to disease. Ann N Y Acad Sci 2008;1124:1–38.

52. Ku J, Lee YS, Chang H, et al. Default mode network disturbances in restless legs syndrome/Willis-Ekbom disease. Sleep Med 2016;23: 6–11.

53. Yoshida T, Mori T, Yamazaki K, et al. Relationship between regional cerebral blood flow and neuropsychiatric symptoms in dementia with Lewy bodies. Int J Geriatr Psychiatry 2015;30:1068–1075.

54. May A. Pearls and pitfalls: neuroimaging in headache. Cephalalgia 2013;33:554–565.